Spin resolved photoelectron microscopy using a two-dimensional spin-polarizing electron mirror

C. Tusche,[1,a)] M. Ellguth,[1] A. A. Ünal,[1] C.-T. Chiang,[1] A. Winkelmann,[1] A. Krasyuk,[1] M. Hahn,[2] G. Schönhense,[2] and J. Kirschner[1]
[1]*Max-Planck-Institut für Mikrostrukturphysik, Weinberg 2, D-06120 Halle, Germany*
[2]*Johannes Gutenberg Universität Mainz, Staudinger Weg 7, D-55128 Mainz, Germany*

(Received 6 April 2011; accepted 27 June 2011; published online 21 July 2011)

We report on an imaging spin-filter for electrons. The specular reflection of low-energy electrons at the surface of a tungsten single crystal is used to project a spin-filtered two-dimensional image onto a position sensitive detector. Spin-filtering is based on the spin-dependent reflectivity of electrons due to spin-orbit coupling in the scattering target, while a two-dimensional field of view, encoded in the angle of incidence, is conserved in the outgoing beam. We characterize the efficiency of the spin-filter by recording photoelectron emission microscopy images of the magnetic domain structure of 8 monolayers cobalt grown on copper (100). © *2011 American Institute of Physics*. [doi:10.1063/1.3611648]

Magnetic imaging by electron microscopy aims at the spatial mapping of the magnetization in micro-structured solid state systems. In particular, photoelectron emission microscopy[1] (PEEM) is a powerful tool for the study of magnetic micro-structures. For instance, the element-selective, as well as magnetically sensitive, core level absorption of polarized soft-X-rays was used to study magnetic interfaces or magnetization dynamics.[2–4] These prototypical systems, confined in one or more dimensions in space, often exhibit unique electronic and magnetic properties, and detailed information on the local spin-dependent electronic structure is fundamental for understanding the underlying physics.

A more direct approach to study magnetic structures is the analysis of the spin of the photoelectrons forming the image. In photoelectron spectroscopy as a general method to analyze the electronic structure of materials, the electron spin is measured by scattering at a solid state target, where scattering cross-sections differ for electrons with opposite spin. Typical configurations include high energy scattering in the Mott detector,[5] spin polarized low energy electron diffraction (SP-LEED),[6] and low energy exchange scattering.[7]

However, a technical limitation common to all existing spin-analyzers is the requirement of sequential measurement of one point in energy-, momentum-, and real-space at a time. While this constitutes no problem to scanning techniques like the scanning electron microscope with polarization analysis (SEMPA),[8] no efficient photoelectron spin-filter for parallel imaging electron microscopes is available, so far.

Here, we report on an innovative spin detector, featuring a simultaneous spin-filtering over a two-dimensional (2D) field of view. The 2D spin-filter is based on the spin dependent reflection, due to spin-orbit coupling, in the (00)-LEED spot at a W(100) single crystalline surface. Scattering takes place at an angle of incidence of 45° with the spin quantization axis oriented normal to the scattering plane.[9] The 2D spin-filter is installed in our "momentum microscope." This instrument combines a PEEM column with an aberration corrected electrostatic energy analyzer with an energy resolution of 200 meV. A detailed description of this instrument is published elsewhere.[10] The spin-filter is inserted into the electron optical path directly after the energy analyzer.

The working principle of the spin-filter is outlined in Fig. 1. After the energy analyzer, an electrostatic retarding lens decelerates the electrons from the pass energy, 100 eV, to the scattering energy, E_{Scatt}, in the range from 15 eV to 90 eV. A reciprocal image is formed at the W(100) scattering target, such that electrons originating from the same point in the spatial image arrive as a parallel beam at the crystal surface. Thus, the spatial information is encoded in the angle of incidence and is conserved upon specular reflection. After a mirror-like 90° reflection, the spatial image is recovered by a second, symmetrical, retarding lens. The spin-integrated direct image still can be obtained by retracting the crystal from the optical path. In both branches, identical electron optics project the image onto the multichannel plate (MCP) of a position sensitive detector.

PEEM images were recorded from 8.0 ± 0.3 monolayer (ML) thick cobalt films using two-photon photoemission (2PPE) by 3.1 eV *p*-polarized light from the second harmonic of a pulsed Ti:Sa laser (pulse length 20 fs and repetition rate 80 MHz). The Co films were grown by thermal

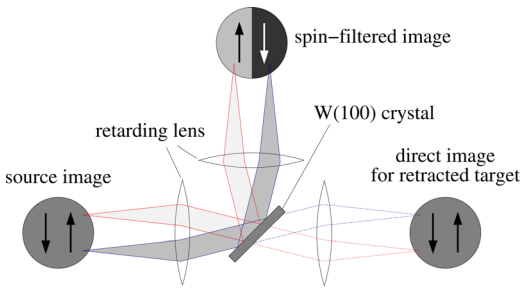

FIG. 1. (Color online) Scattering geometry for the specular reflection of electrons at the W(100) crystal. Scattering takes place under parallel beam conditions, preserving the spatial information of the source image. The spin-integrated image is obtained by retracting the W(100) crystal.

[a)]Electronic mail: tusche@mpi-halle.mpg.de.

evaporation from a high purity Co rod onto a clean Cu(100) single crystal at a temperature of 400 K. Before the measurements, the W(100) scattering target was prepared by standard procedures[11] to obtain a clean and carbon free surface.

The as-grown Co film does not show a contrast in the non-spin-filtered PEEM image. By inserting the W(100) analyzer into the optical path, contrast is obtained at $E_{\mathrm{Scatt}} = 27$ eV, showing dark and bright domains of a random magnetic structure. Similar patterns were observed previously by SEMPA for Co films of comparable thickness.[8] In our experiments, the sample was not demagnetized, and the initial magnetization alignment is likely to be influenced by residual magnetic fields during growth. We find maximum contrast, *i.e.*, opposite magnetization directions in two domains, when the ⟨100⟩ directions are aligned vertical, along the quantization axis of the spin-filter. Figure 2(a) shows an overview image of two domains imaged by photoelectrons from 0.3 eV below the Fermi level. The color scale directly corresponds to measured intensities. The image was integrated over a time of 120 s while the laser focus ($\varnothing = 20\ \mu$m) was periodically scanned over the imaged area.

We compare the observed domain pattern to images obtained by magnetic circular dichroism (MCD) (Refs. 12 and 13) in 2PPE. Ten consecutive images with an integration time of 60 s were taken for left- and right-circular polarization of the light, resulting in a measurement time of 20 min. Figure 2(b) shows the asymmetry of the same area as in Fig. 2(a). The scale bar on the right is given by $A = [I^+ - I^-]/[I^+ + I^-]$, with the intensity $I^{\pm}$ for left- and right-circular polarized light. Note, that the sample was rotated by 60° during the measurement in order to obtain a non-vanishing projection of the magnetization component onto the propagation direction of the light.

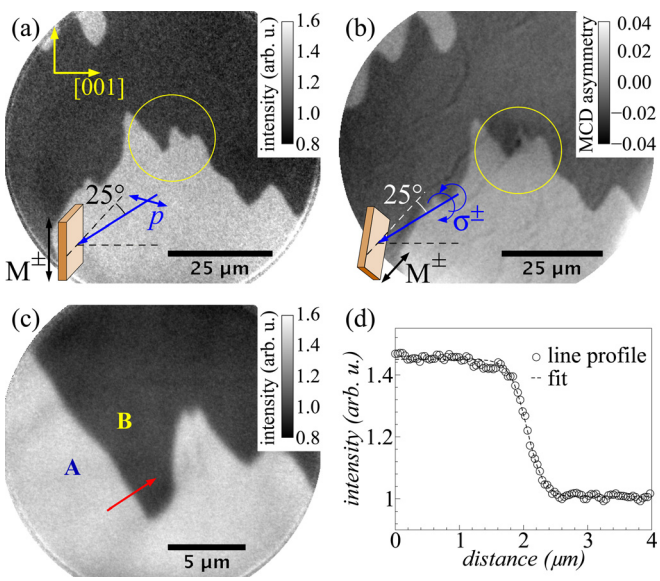

FIG. 2. (Color online) (a) Spin-filtered image of the 8 ML Co film observed after the electron beam was scattered at the W(100) crystal. (b) The same domains imaged by MCD. (c) A high magnification image of the area marked in (a) and (b). (d) Intensity profile across the domain wall between areas A and B. The inset in (a) and (b) shows the relative orientation of the sample, the propagation direction and polarization of the light, and the magnetic quantization axis ($M^{\pm}$).

Figure 2(c) shows a detail of the magnetic domain boundary, marked in Figs. 2(a) and 2(b). Sharp contours of the domains could be observed with a 46% intensity variation. The lateral image resolution was extracted from an intensity-profile across the domain wall, along the displayed line. The intensity plot is shown in Fig. 2(d) together with a fit to the analytical solution for a 180° domain wall with uniaxial anisotropy, which is a hyperbolic tangent profile. We derive a width of the domain wall in the image of 500 ± 30 nm. However, we note that this value does not represent directly the instrumental resolution of the 2D spin-filter. For instance in Ref. 14, the domain wall width of a 5.5 ML film and of a 9 ML film was found to be 600 nm and 400 nm, respectively. By observing a 20% larger width for the 8 ML film, we conclude that the instrumental image resolution is better than 300 nm, including aberrations of the electron optics.

In Fig. 3, we show the intensity observed in domains A and B as a function of E_{Scatt}, as well as the resulting scattering asymmetry, defined as above with the intensity, $I^{\pm}$, in the two domains. In the energy range from 15 eV to 90 eV, the observed intensity varies over two orders of magnitude. At the same time, the asymmetry shows an oscillatory behavior. In particular, we find pronounced maxima with $A = 0.19$ at $E_{\mathrm{Scatt}} = 27$ eV and $A = 0.20$ at $E_{\mathrm{Scatt}} = 71$ eV and large negative asymmetry, $A = -0.22$, at $E_{\mathrm{Scatt}} = 64$ eV. At the first asymmetry maximum, at $E_{\mathrm{Scatt}} = 27$ eV, the intensity is near to its maximum as well. This is the preferred working point for the 2D spin-filter, also used in the measurements of Fig. 2.

For a measured asymmetry, the electron spin-polarization is given by $P = \frac{1}{S}A$, where S is the characteristic Sherman function of the spin-filter. For the Co/Cu(100) sample, the spin-polarization of electrons emitted in 2PPE is well known. A spin-polarization between 40% and 50% in 2PPE from 0.3 eV below the Fermi level is reported in the literature for thick Co films.[15] In our laboratory, we obtain a value around 45% measured for 6–7 ML of cobalt films, using a well characterized spin-detector.[7] With these values, we derive S from the domain contrast in Fig. 2(c) at $E_{\mathrm{Scatt}} = 27$ eV and obtain $S = 0.42 \pm 0.05$ for the 2D spin-filter.

The efficiency of a single channel spin-detector is expressed by the figure-of-merit, $f_0 = S^2 \frac{I}{I_0}$, with the spin average reflectivity $\frac{I}{I_0}$, and accounts for the acquisition time needed to get the same statistical error of a single data point as compared to the spin-integrated experiment. With

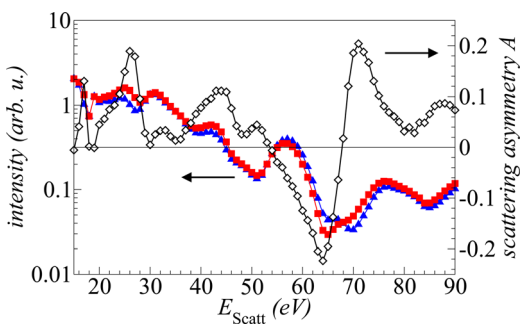

FIG. 3. (Color online) The reflected intensity in domains A (▲) and B (■) as in Fig. 2, plotted on a logarithmic scale, and the calculated asymmetry (◊) as a function of E_{Scatt}.

$S = 0.42$ and $\frac{I}{I_0} = 1.2\%$, measured by the MCP count rates, we obtain $f_0 = 2.1 \cdot 10^{-3}$. We find that this efficiency, calculated for a single point, is higher than the f_0 of most of the available single-channel detectors[5–7] with $f_0 = 10^{-3}$ to 10^{-4}. However, typical data sets like a photoelectron spectrum or a PEEM image consist of multiple points. Such 2D electron distributions can be measured sequentially using a single-channel detector, *i.e.*, by placing a movable aperture in the plane of the PEEM image.[16] Then, the acquisition time for the data set is given by the time for a single point multiplied by the number of points. By contrast, simultaneous measurement of N independent channels reduces the total acquisition time by the factor N, using the same f_0.

One can define the efficiency of the 2D spin-filter by the rate at which data points are collected. As for f_0, the statistical error should be comparable to a spin-integrated point acquired for time t_0. With the spin-resolved acquisition time t, the data rate is N/t, and we define the 2D detection efficiency by $\mathcal{F}_{2D} = \frac{t_0}{t} N = f_0 N$. In our experiments, we can distinguish 70 discrete points over the diameter of the PEEM image, calculated on the basis of the resolution of Fig. 2(c). This results in $N = 3800$ parallel recorded channels, and we get $\mathcal{F}_{2D} \approx 8.0$. A single-channel detector with $N = 1$ will have a $\mathcal{F}_{2D} = f_0$. We therefore can directly compare the efficiency to record a 2D image using different detectors. For instance, this measurement is $8 \cdot 10^4$ times faster than the measurement of the same 2D image data using a Mott detector[5] with $f_0 = 1 \cdot 10^{-4}$ in scanning mode. The increased efficiency is related to both, the parallel recording of 3800 channels and a higher f_0 for each channel.

As pointed out, a crucial parameter for the 2D efficiency is the number N of resolvable points. Here, N is limited by the angular resolution of the electron diffraction process. In contrast to a typical LEED experiment where the angular resolution is usually limited by the energy width and divergence of the primary beam, here, each image point is the source of an ideally parallel beam. We further use diffraction in the (00)-LEED spot. Unlike all other LEED spots, the momentum transfer vector is oriented normal to the surface. Therefore, the angle of the diffracted beam is independent of the energy, and $\Delta E = 200$ meV will not cause angular broadening. The fundamental limitation of the image resolution, however, is imposed by the crystal quality of the target. For a tungsten crystal a mosaic-spread of 0.05°–0.1° is a typical value, *i.e.*, a parallel beam will be diffracted into a cone of a width $\leq 0.1°$. After projection onto the MCP, this translates into ≥ 60 resolvable diagonal points. This estimation shows that the experimentally observed resolution is in good agreement with what can be expected for a tungsten crystal. The resolution might be considerably increased when a target with a smaller mosaic-spread could be used.

In summary, we demonstrated spin-filtering of two-dimensional images by low energy specular reflection of electrons at a W(100) surface. Due to the parallel detection scheme, the spin-filter is ideally suited for applications in spin-resolved electron microscopy and time-resolved studies. Magnetic imaging by mapping the spin polarization of photoelectron is found to be comparable to measurements by magnetic circular dichroism, however, with a ten times shorter acquisition time. Spin-filtering is not limited to spatial images, but also possible in energy and momentum resolved imaging.[10] The latter allows recording of the spin-resolved angular distribution of photoelectrons and will be the subject of further studies.

We would like to thank M. Escher and N. Weber from Focus GmbH for the electron optical design and construction of the 2D spin-filter.

[1]E. Bauer, J. Phys.: Condens. Matter **21**, 314001 (2009).
[2]H. Ohldag, T. J. Regan, J. Stöhr, A. Scholl, F. Nolting, L. J. C. Stamm, and R. L. White, Phys. Rev. Lett. **87**, 247201 (2001).
[3]J. Vogel, W. Kuch, M. Bonfim, J. Camarero, Y. Pennec, F. Offi, K. Fukumoto, J. Kirschner, A. Fontaine, and S. Pizzini, Appl. Phys. Lett. **82**, 2299 (2003).
[4]A. Krasyuk, A. Oelsner, S. Nepijko, A. Kuksov, C. Schneider, and G. Schönhense, Appl. Phys. A **76**, 863 (2003).
[5]D. Pierce, R. Celotta, M. Kelley, and J. Unguris, Nucl. Instrum. Methods Phys. Res. A **266**, 550 (1988).
[6]D. Yu, C. Math, M. Meier, M. Escher, G. Rangelov, and M. Donath, Surf. Sci. **601**, 5803 (2007).
[7]A. Winkelmann, D. Hartung, H. Engelhard, C.-T. Chiang, and J. Kirschner, Rev. Sci. Instrum. **79**, 083303 (2008).
[8]H. Oepen, M. Benning, H. Ibach, C. Schneider, and J. Kirschner, J. Magn. Magn. Mater. **86**, L137 (1990).
[9]J. Kirschner and R. Feder, Phys. Rev. Lett. **42**, 1008 (1979).
[10]B. Krömker, M. Escher, D. Funnemann, D. Hartung, H. Engelhard, and J. Kirschner, Rev. Sci. Instrum. **79**, 053702 (2008).
[11]K. Zakeri, T. Peixoto, Y. Zhang, J. Prokop, and J. Kirschner, Surf. Sci. **604**, L1 (2010).
[12]K. Hild, J. Maul, G. Schönhense, H. J. Elmers, M. Amft, and P. M. Oppeneer, Phys. Rev. Lett. **102**, 057207 (2009).
[13]T. Nakagawa, K. Watanabe, Y. Matsumoto, and T. Yokoyama, J. Phys.: Condens. Matter **21**, 314010 (2009).
[14]A. Berger and H. P. Oepen, Phys. Rev. B **45**, 12596 (1992).
[15]O. Andreyev, Y. M. Koroteev, M. Sánchez Albaneda, M. Cinchetti, G. Bihlmayer, E. V. Chulkov, J. Lange, F. Steeb, M. Bauer, P. M. Echenique, S. Blügel, and M. Aeschlimann, Phys. Rev. B **74**, 195416 (2006).
[16]F. Kronast, J. Schlichting, F. Radu, S. Mishra, T. Noll, and H. Dürr, Surf. Int. Anal. **42**, 1532 (2010).